MARTIN MARIETTA ENERGY SYSTEMS LIBRARIES
3 4456 0139078 8

ORNL/TM-10049

ornl

OAK RIDGE NATIONAL LABORATORY

MARTIN MARIETTA

Design, Construction, and Initial Results for an Erosion-Corrosion Test System

J. R. Keiser

OAK RIDGE NATIONAL LABORATORY
CENTRAL RESEARCH LIBRARY
CIRCULATION SECTION
4500N ROOM 175
LIBRARY LOAN COPY
DO NOT TRANSFER TO ANOTHER PERSON
If you wish someone else to see this report, send in name with report and the library will arrange a loan.

OPERATED BY
MARTIN MARIETTA ENERGY SYSTEMS, INC.
FOR THE UNITED STATES
DEPARTMENT OF ENERGY

Printed in the United States of America. Available from
National Technical Information Service
U.S. Department of Commerce
5285 Port Royal Road, Springfield, Virginia 22161
NTIS price codes: Printed Copy: A03 Microfiche: A01

This report was prepared as an account of work sponsored by an agency of the United States Government. Neither the United States Government nor any agency thereof, nor any of their employees, makes any warranty, express or implied, or assumes any legal liability or responsibility for the accuracy, completeness, or usefulness of any information, apparatus, product, or process disclosed, or represents that its use would not infringe privately owned rights. Reference herein to any specific commercial product, process, or service by trade name, trademark, manufacturer, or otherwise, does not necessarily constitute or imply its endorsement, recommendation, or favoring by the United States Government or any agency thereof. The views and opinions of authors expressed herein do not necessarily state or reflect those of the United States Government or any agency thereof.

ORNL/TM-10049

Metals and Ceramics Division

DESIGN, CONSTRUCTION, AND INITIAL RESULTS FOR AN EROSION-CORROSION TEST SYSTEM

J. R. Keiser

Date Published: May 1986

NOTICE: This document contains information of a preliminary nature. It is subject to revision or correction and therefore does not represent a final report.

Research sponsored by the U.S. Department of Energy,
Advanced Research and Technology Development
Fossil Energy Materials Program

Prepared by the
OAK RIDGE NATIONAL LABORATORY
Oak Ridge, Tennessee 37831
operated by
MARTIN MARIETTA ENERGY SYSTEMS, INC.
for the
U.S. DEPARTMENT OF ENERGY
under Contract No. DE-AC05-84OR21400

MARTIN MARIETTA ENERGY SYSTEMS LIBRARIES
3 4456 0139078 8

CONTENTS

ABSTRACT 1
INTRODUCTION 1
EXPERIMENTAL SYSTEM 2
OVERVIEW 2
EROSIVE-PARTICLE GUN 3
VELOCITY MEASUREMENT SYSTEM 6
GAS PULSE DEVICE 7
HOT STAGE 8
GAS FLOW CONTROL SYSTEM 9
TURBOMOLECULAR PUMP 11
IMAGE ENHANCEMENT SYSTEM 11
OTHER MODIFICATIONS 12
COMPLEMENTARY EQUIPMENT 12
INITIAL RESULTS 13
SUMMARY 16
REFERENCES 18

DESIGN, CONSTRUCTION, AND INITIAL RESULTS FOR AN EROSION-CORROSION TEST SYSTEM*

J. R. Keiser

ABSTRACT

Erosion and erosion-corrosion are among the most serious forms of material degradation encountered in coal conversion and combustion systems. To improve our understanding of such phenomena, a unique system has been constructed to perform erosion and erosion-corrosion studies in a specially modified scanning electron microscope. This microscope incorporates a gun that shoots erosive particles at a target specimen and also a hot stage that can heat both the test specimen and a corrosive gas directed onto the specimen surface. Initial results show that the system is capable of novel studies of erosion and erosion-corrosion, which should lead to improved understanding of those degradation modes.

INTRODUCTION

Erosion and erosion-corrosion can cause considerable material degradation in systems such as gas turbines and coal conversion systems, so many researchers have studied those problems. Generally the work is performed with a gas gun, which directs a gas stream loaded with solids onto the target. The erosive particles are approximately the size of particles in the systems of interest. Because many grams and even hundreds of grams of particles strike the surface before the surface is examined, only cumulative effects are measured; little or nothing is learned about the response of the target material to individual impacts.

Studies in which single particles are used to investigate the basic deformation response of the target have employed particles considerably

*Research sponsored by the U.S. Department of Energy, AR&TD Fossil Energy Materials Program [DOE/FE AA 15 10 10 0, Work Breakdown Structure Element ORNL-3(C)] under contract DE-AC05-84OR21400 with Martin Marietta Energy Systems, Inc.

larger than those found in the systems of interest. Consequently it is not clear that the material behavior observed in the experiments is characteristic of that under impacts by much smaller particles.

An additional shortcoming of most work performed up to this time is that material reacted at elevated temperature is not examined until it has cooled. The change in temperature can result in spallation of scales or in a phase change, so the material examined at room temperature is not necessarily representative of that existing at operating conditions of the systems of interest.

We have constructed a system that permits studies of the impact effects of single particles of the size found in coal conversion systems. Furthermore, the test samples can be examined at temperature and under corrosive conditions with a scanning electron microscope.

EXPERIMENTAL SYSTEM

OVERVIEW

The experimental system is based on an ISI Super IIIA scanning electron microscope* (SEM) specially modified to permit in-situ studies of the erosion, corrosion, and erosion-corrosion characteristics of metallic or ceramic surfaces. The major additions to the SEM are a gun, which shoots individual particles at a sample at high velocity, and a hot stage, which heats the specimen and the corrosive gas and directs the gas onto the sample surface.

The velocity of the erosive particles fired from the gun is measured by a photoelectric timing device in the gun barrel. The particles are propelled by pulses of gas, which are regulated by a specially built device that controls the duration of electrical pulses to the solenoid valve. The propellant gas is rapidly removed from the SEM chamber by a turbomolecular pump that supplements the standard SEM pumping system.

A commercial gas flow control system delivers a stream of corrosive gas to the specimen surface. Diffusion of this gas into the SEM filament area is minimized by rapid removal of the gas with the turbomolecular pump.

---

*Manufactured by International Scientific Instruments, Inc., Milpitas, Calif.

During elevated-temperature operations and corrosion studies, rapid acquisition of a high-quality image is imperative. Because operation at high temperature or increased gas pressure can degrade the image and because the SEM camera requires at least three minutes per picture, an image enhancement system was added to the SEM to permit rapid acquisition of images whose quality is considerably better than those obtained in the normal manner.

EROSIVE-PARTICLE GUN

One of the most significant additions to the SEM is a gas gun that propels 0.343-mm-diam (0.0135-in.) tungsten carbide balls. Many researchers have built guns to shoot particles; however, most have been designed for larger balls or for multiple-particle shots.[1,2] The current design was twice modified to improve the method of reloading and bringing the next ball into firing position. The first design incorporated a spring-activated reloading mechanism and a cylinder that rotated on an axis perpendicular to the barrel. Although balls were successfully fired from this gun, the reloading mechanism never worked satisfactorily. The second design had a dovetailed sliding connection to move balls from a spring-loaded ball holder into the firing chamber (Fig. 1). This gun was used for the initial experimental studies, but, as with the first design, reloading was a problem. The barrels of the first two guns were fabricated from type 304 stainless steel hypodermic tubing [0.635 mm (0.025 in.) outside diam, 0.330 mm (0.013 in.) inside diam]. The gun bodies were machined from brass.

The third and latest gun is easier to reload and has a built-in velocity measurement system. This gun, shown in Fig. 2, is built on a flange that mounts directly on the SEM chamber. On the outside of the flange are the gas inlet tube, a 14-pin electrical connector for communication with the control and measurement panel, and a rotating knob for advancing a ball into firing position. On the inside of the flange, the teeth of a gear can be seen between two brass plates. This gear is rotated by a gear connected to the hand knob. As shown in Fig. 3, it rotates to position the projectile between the gas supply tube and the gun barrel. The gear has 40 precisely drilled holes arranged in two concentric rings of 20 holes each. The outer ring acts as an alignment guide for positioning the projectiles,

ORNL-DWG 83-18069R

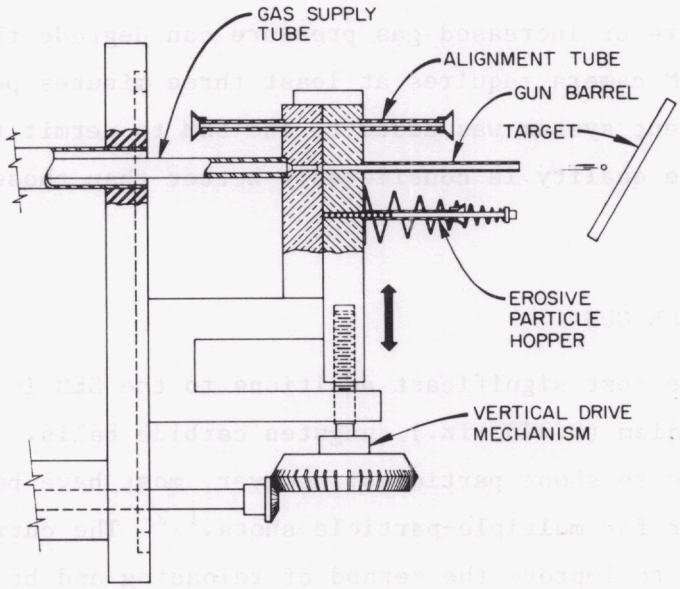

Fig. 1. Schematic drawing of the second version of the erosive-particle gun.

Y202280

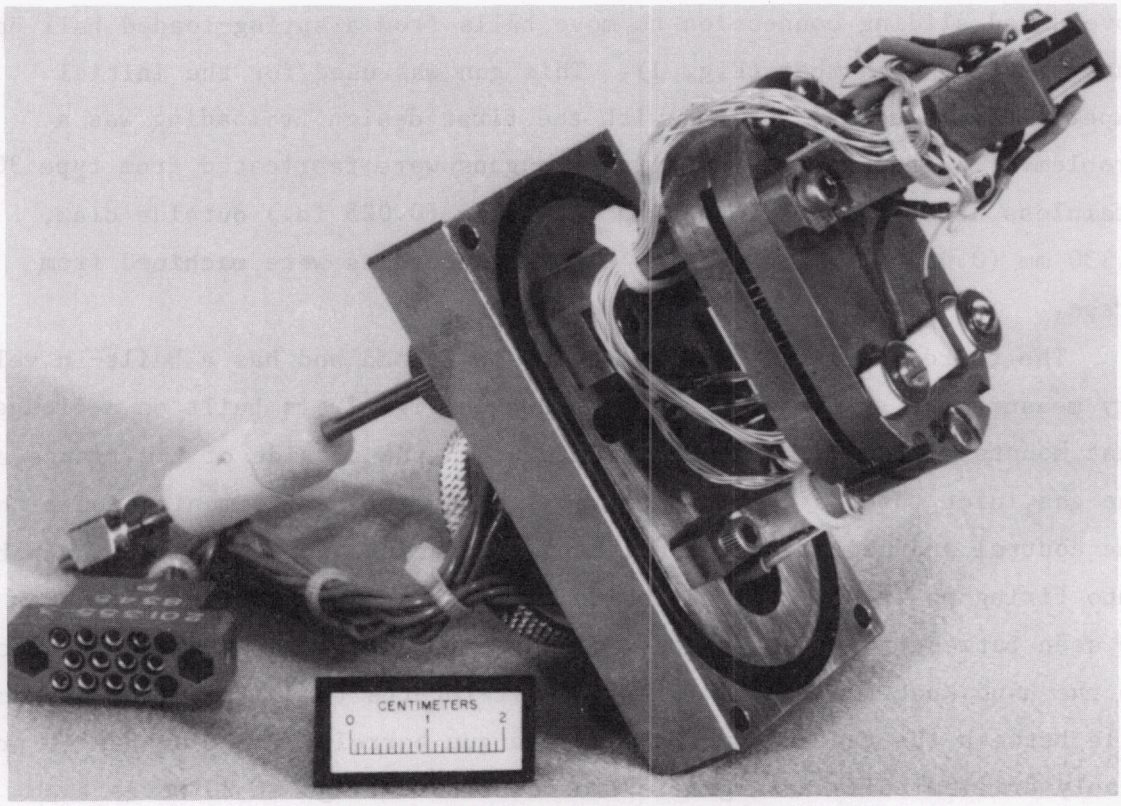

Fig. 2. Erosive-particle gun currently in use.

ORNL-DWG 86-7609

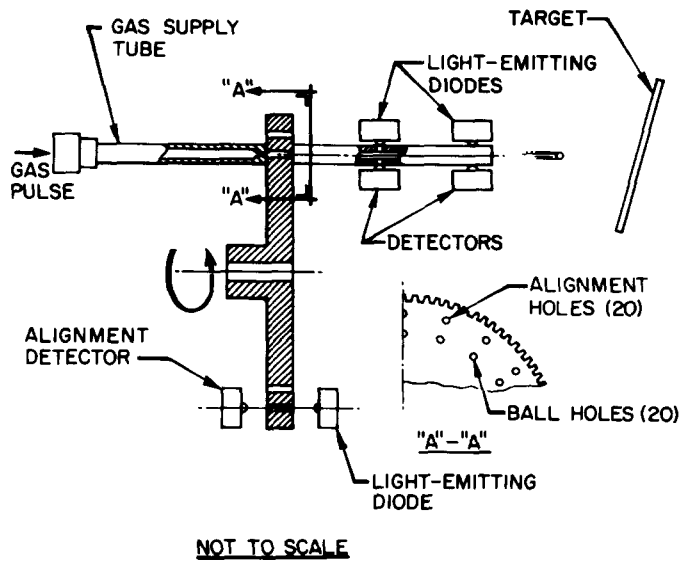

Fig. 3. Schematic drawing of the currently used erosive-particle gun.

while the inner ring carries the projectiles, i.e., serves as a 20-shot revolver cylinder. A light-emitting diode and photon collector located near the bottom of the gun are used to position the gear so that a hole (on the inner ring) brings a projectile into alignment with the gas supply tube and gun barrel, which are exactly 180° away from the bottom hole. Proper positioning is indicated when the signal from the collector is maximized as indicated by a meter on the control panel.

A charge of gas of controlled pressure and duration projects the ball through the barrel. Carbon dioxide has been used as the propellant gas. It has the advantage that the ambient equilibrium pressure between gaseous and liquid carbon dioxide in the gas cylinder [about 6.4 MPa (930 psi)] cannot exceed the maximum pressure for solenoid valve operation, thus providing a safeguard against regulator failure. For the same pressure, higher projectile velocities could be attained by using gases of lower molecular weight,[1] so, if higher velocities are needed, a lighter propellant gas will be adopted. If lower velocities are desired, lower carbon dioxide pressures are used. Particle velocities used in experimental studies are generally in the range 15 to 45 m/s (50–150 ft/s), but velocities as high as 90 m/s (300 ft/s) have been attained.

The tip of the barrel is visible in Fig. 2, which also shows the wiring harness and printed circuit (pc) boards that are mounted on the brass piece that supports the barrel. This wiring harness and the pc boards are the main components of the velocity measurement system, which is described below. The barrel for this gun was fabricated from type 316 stainless steel capillary tubing [1.59 mm (0.0625 in.) outside diam, 0.254 mm (0.010 in.) inside diam]. The inside diameter is enlarged by drilling to be slightly larger than ball diameter. The other large pieces of the gun, including the large gear, are made of brass.

The gun is firmly attached to the SEM sample chamber, and the specimen holder and hot stage are tilted to change the angle of impact of the erodent particles on the specimen surface. The impact angle can be varied from 10 to 90° (at 90° the plane of the specimen surface is normal to the flight path of the erodent particles).

As built, this gun shoots standard 0.343-mm-diam (0.0135-in.) tungsten carbide balls, which are purchased from a ball bearing manufacturer. Cobalt-bonded tungsten carbide is used because of its high hardness. The 0.343-mm size was chosen because of the limited availability of smaller sizes and because formidable machining difficulties would be encountered in building a gun for much smaller balls.

VELOCITY MEASUREMENT SYSTEM

It is essential to know the velocity of a ball when it strikes the target in order to relate the impact damage to the momentum or kinetic energy. A time-of-flight device was designed by engineers in the ORNL Instrumentation and Controls Division to record the travel time of the projectile over a fixed distance through the barrel. Light beams from two light-emitting diodes separated by 25.4 mm (1.00 in.) are directed through a pair of aligned narrow holes in the barrel and into a collector. Interruption of the light beam by a particle causes a pulse in the electrical signal from the collector. This is a commonly used technique, and the design and construction of such a timing device would be straightforward if it were not for the small size of the balls. To ensure that the column of light is completely shadowed by the ball as it passes through the

barrel, the light shaft is confined to 0.25 mm diam (0.010 in.). This results in a relatively small steady-state source of light energy reaching the collector; consequently, the electrical current signal is relatively weak. In addition, a ball traveling 30 m/s totally interrupts the light beam for only about 10 μs; thus, the electrical signal pulse is very short. Because of these conditions, fast high-gain preamplifiers are required to convert the start and stop current signals into signals that can be used to control digital time-of-flight measurement circuitry. The time between the detection of the first and second pulses is measured by using the pulses to start and stop a 1-MHz clock that is connected to a counter. The resulting count divided by the 1-MHz clock rate equals the particle's time of flight with ∓1-μs accuracy. The velocity (V_f) is then determined from the time of flight (t_f) and the separation distance of the diodes (d_s):

$$V_f = d_s/t_f \ .$$

GAS PULSE DEVICE

Gases introduced into the SEM can cause damage to the filament used to supply electrons for the microscope and can cause focusing problems. Although extra pumping capacity* has been added to this system, it is desirable to keep the amount of gas introduced into the sample chamber to a minimum when the gun is fired. Therefore, it is important to limit the duration of the gas pulse used to propel the projectile. This requires a fast-acting solenoid valve to open and close the gas supply and an equally fast electronic circuit to control the electrical pulse to the solenoid. The present circuit provides a short-duration, higher-voltage signal to open the valve quickly and then maintains a lower-voltage output to hold the valve open for a preset time. For most applications, the full pulse duration is 15 ms, although the duration can be varied from 5 to 1000 ms. Thus, the pulse duration can be optimized to achieve the needed particle velocity with the minimum gas load.

---

*See subsequent discussion of the turbomolecular pump.

HOT STAGE

Hot stages for a SEM with and without the capability to heat and direct a corrosive gas have been described in the literature.[3-6] Our first hot stage, shown in Fig. 4, was fabricated from a machinable glass

Y-201451

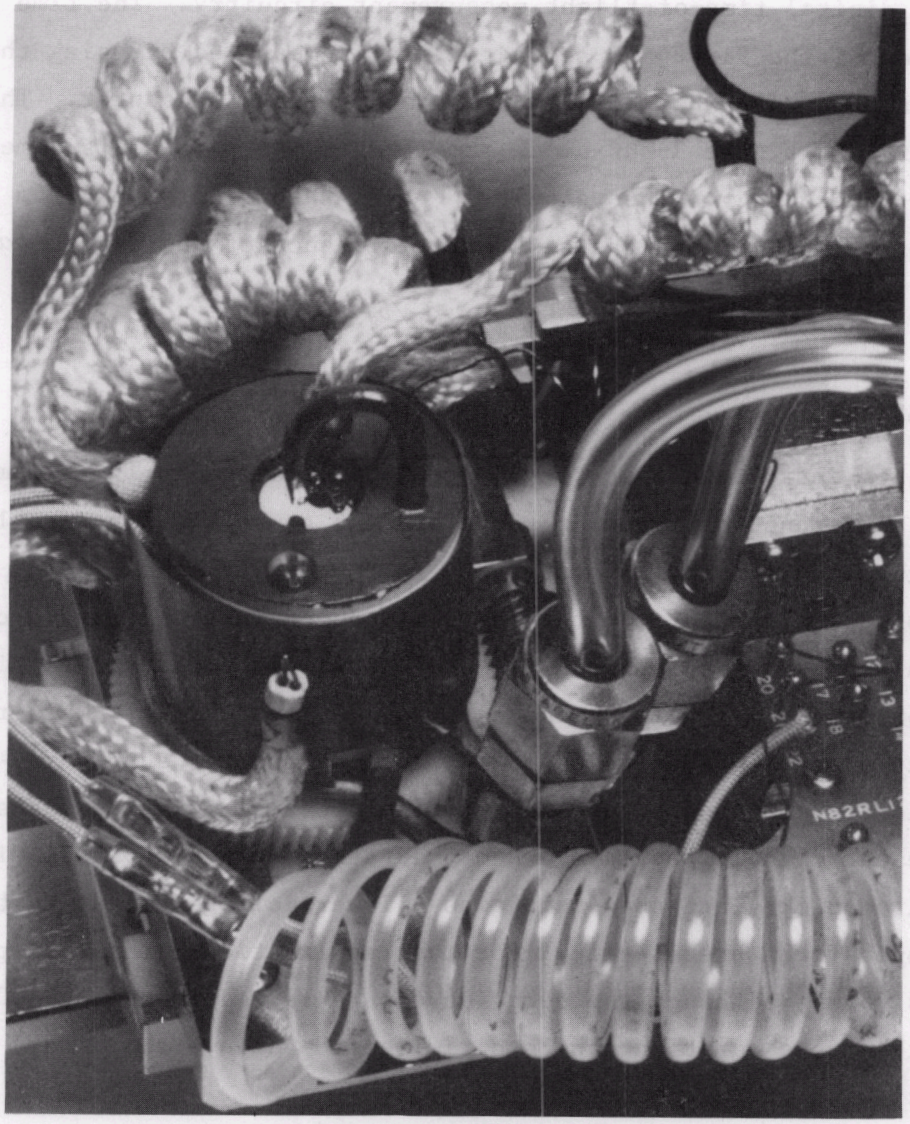

Fig. 4. Original hot stage designed and constructed at ORNL for heating a sample and a corrosive gas for in-situ corrosion studies.

chosen because of its fabricability and relatively good insulating properties. A commercially available* ceramic heater, 12.7 mm in diam (0.5 in.) and 1.59 mm thick (0.0625 in.), provided an upper temperature capability of 700°C. Reactive gases used for corrosion studies were heated by passing them through a channel machined into the body of the hot stage. Both ends of the channel were terminated by a female tapered ground glass joint. Quartz tubes were machined to fit these joints, and the quartz tube at the gas exit was bent into an inverted J shape so that the hot gas could be directed onto the hot surface of a sample mounted on the hot stage. The quartz inlet tube was connected to a coil of plastic tubing that led to a gas feedthrough on the SEM door. The hot stage was equipped with four chromel-alumel thermocouples to measure the sample temperature, control the heating element, and monitor the temperature in two locations at the base of the hot stage.

During early studies with the hot stage, it was found necessary to add a cooling system that would maintain the SEM stage mounting disk at an acceptable temperature to accommodate adjacent nylon gears. The original brass disk was replaced with a copper disk to which was brazed a coil of copper tubing 3.18 mm (0.125 in.) in outside diameter. Flexible coils of plastic tubing connected the copper cooling coil to feedthroughs on the SEM door. Air or water was passed through this cooling coil.

A new hot stage was fabricated to our specifications by a SEM equipment supplier.† This hot stage, shown in Fig. 5, includes a gas preheating system similar to that on the first hot stage and a water-cooled copper heat sink. It is capable of operation at temperatures of at least 1100°C (2012°F).

GAS FLOW CONTROL SYSTEM

The supply of corrosive gas to the hot stage is regulated with a commercial gas flow control system. This system uses a flow measuring transducer that gives a signal to a controller. The controller compares the flow rate measured with the controller flow rate setting and then adjusts a solenoid valve to give the desired flow rate. Because only a very small volume of gas is needed (typical flow rates are 2–8 cm^3/min), the flow

---

*Hittman Materials & Medical Components, Inc., Columbia, Md.

†Ernest F. Fullam, Inc., Latham, N.Y.

YP1888

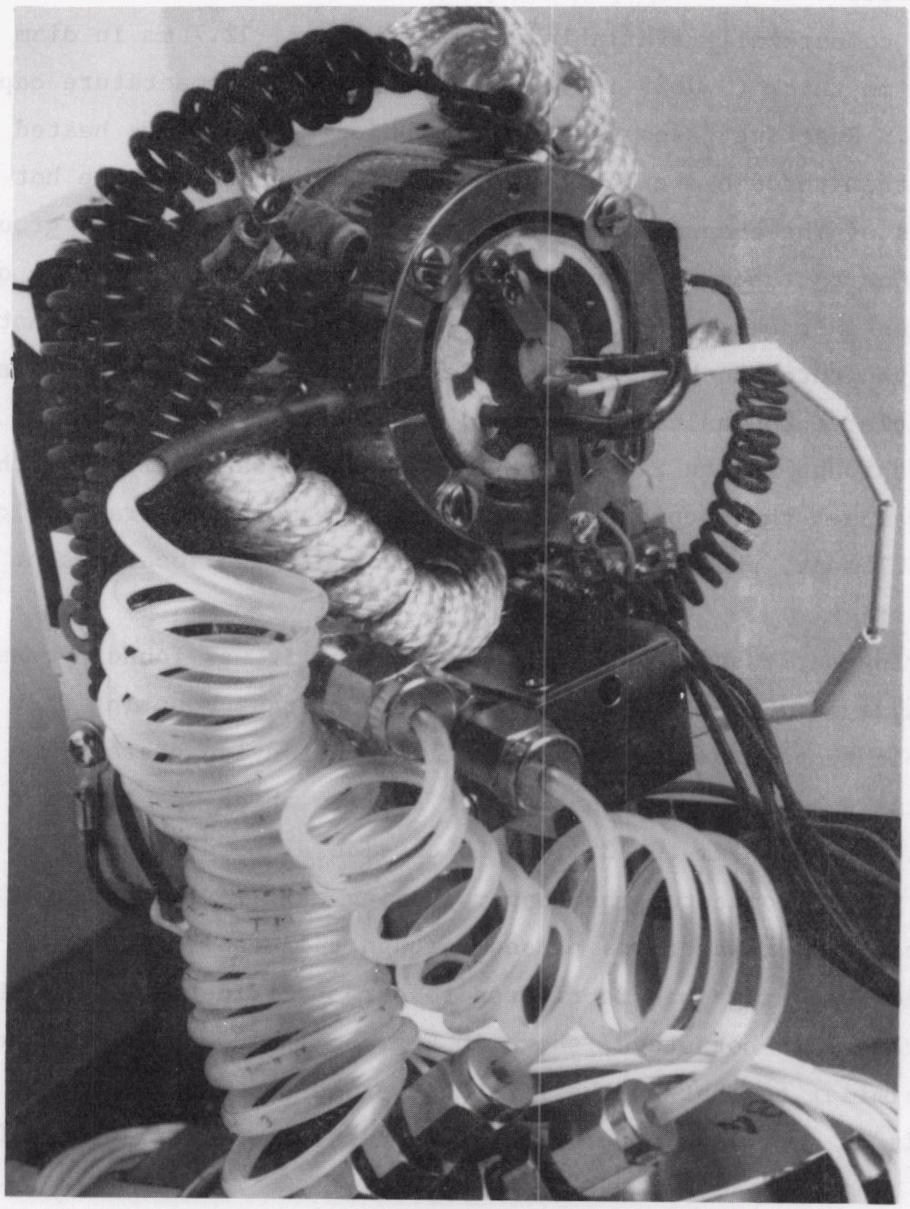

Fig. 5. Hot stage purchased from Ernest F. Fullam, Inc., with capability for operation at 1100°C.

transducers used were the smallest-capacity units commercially available. The partial pressure of the corrosive gas at the sample surface is estimated from a form of the Hertz-Langmuir equation used by Rapp:[4]

$$J_{max} = A\, P_i/(2\, \pi\, RTM_i)^{1/2} ,$$

where

J_{max} = molecular flow rate (mole/sec),
P_i = gas pressure (dynes-cm^{-2}),
M_i = molecular weight of gas (g-mole^{-1}),
R = gas constant (8.31432×10^7 g cm^2 sec^{-2} mol^{-1} K^{-1}),
T = temperature (K),
A = exposed area (cm^2).

TURBOMOLECULAR PUMP

The turbomolecular pump, Balzers model TPU-330,* was added to the system to rapidly remove gases introduced into the microscope when the gun is fired or when corrosive gas is used during in-situ corrosion studies. The turbomolecular pump used has a rated nitrogen pumping capacity of 300 L/s and permits continuous operation of the SEM during corrosion studies. To attach the pump to the SEM, a 51-mm-diam (2-in.) hole was cut in the right side of the sample chamber (the side opposite the mounting location of the SEM detector tube and the erosive particle gun), and a large-diameter vacuum-tight tube was connected to the pump. A bellows was included to aid vibration damping.

IMAGE ENHANCEMENT SYSTEM

A Crystal† image enhancement system was incorporated to improve the quality of the displayed image and to make a permanent digital record of the image. In addition to standard noise reduction features, this system accepts a slow scan input signal and has the capability to digitally store images on a hard disk. The standard features include signal averaging, integration, crispening, and filtering. In signal averaging, the image displayed on the monitor is a running average over an arbitrarily selected number of frames; this provides an effectively real-time image with greatly reduced noise levels. The integration feature provides a frozen image which is an average taken over an operator-selected number of frames for noise reduction. Crispening and filtering

---

*Manufactured by A. Pfeiffer GmbH, Asslar, Federal Republic of Germany.
†Manufactured by Quantel, Palo Alto, Calif.

features can be used on this frozen image to improve the resolution of surface features. The image storage option allows the Crystal system to digitally store up to 32 of these noise-reduced, edge-enhanced images on a hard disk. Hard copies (photographs) of the stored images can be made from the Crystal monitor or the SEM photographing monitor.

OTHER MODIFICATIONS

The heat radiated into the SEM sample chamber during operation of the hot stage, along with an increased partial pressure of the corrosive gas, can cause degradation of SEM components. The scintillator disk and the final aperture are especially susceptible to declines in performance. Problems with the final aperture are solved by cleaning or replacing the aperture. The problems with the scintillator disks are minimized by using quartz disks with a carbon coating over the phosphor instead of the standard aluminum coating over the phosphor on a glass or plastic disk. This technique was described in more detail by Castle and Hunt.[5]

COMPLEMENTARY EQUIPMENT

Two pieces of experimental equipment (not part of the modified SEM) are being used as accessory tools to provide additional, complementary experimental information. An Alpha-Step 200* profilometer is being used to make a two-dimensional scan of surface features resulting from particle impacts or corrosion. Impact crater depths and diameters can be determined from recorder traces of the profilometer scans, and the height and extent of extruded lips can be estimated. A Nanoindenter,† which is an ultralow-load microindentation apparatus, is used to measure the hardness in and around impact craters. This device performs a constant strain rate indentation test to determine the hardness as a function of depth by measuring the force needed to move the indenter to progressively greater depths.

---

*Manufactured by Tencor Instruments, Mountain View, Calif.

†Nanoindenter Instruments, Inc., Knoxville, Tenn.

INITIAL RESULTS

The system we have described was completed in January 1986. However, we performed several experiments during and subsequent to construction, and considerable information of significant scientific value has been obtained.[7] Because the purpose of this report is to describe the experimental system rather than to provide detailed experimental results, only examples of results will be presented. Detailed explanations of the data and their scientific significance will be provided in subsequent papers.

A ball fired from the gun damages the surface of the target material in a manner determined by the properties of the ball and of the target. For a ductile target material and a ball with sufficient velocity, an impact crater is formed. The impact angle has a strong influence on the crater shape, while the ball velocity and the properties of the ball and target material determine the crater depth. Figure 6 shows impact craters formed by balls striking at 30° and 90°. Both impacts caused extrusion of material from the craters; for the 30° impact, considerable material piled up at the exit end of the crater, while the 90° impact produced a lower mound of material all around the crater.

The dimensions of an impact crater are determined with the profilometer. Figure 7 shows a SEM micrograph of a crater and the profilometer recorder trace of the same crater. Clearly the profilometer data provide better measurements of crater length, crater depth, and lip height than those obtained from SEM micrographs.

A standard microhardness tester makes indentations about the same size as the craters made by the tungsten carbide balls we use. Because we need measurements of the properties of the surface in and around the craters, a small indentation hardness tester was needed. We use the recently developed Nanoindenter[8] to measure the hardness near and at the center of a crater. Recent studies with a nickel-base alloy indicated that the material in the bottom of a crater is generally harder than that on the unaffected surface. Figure 8 shows a 90° impact crater on a nickel-base alloy and the six indentations made by the Nanoindenter.

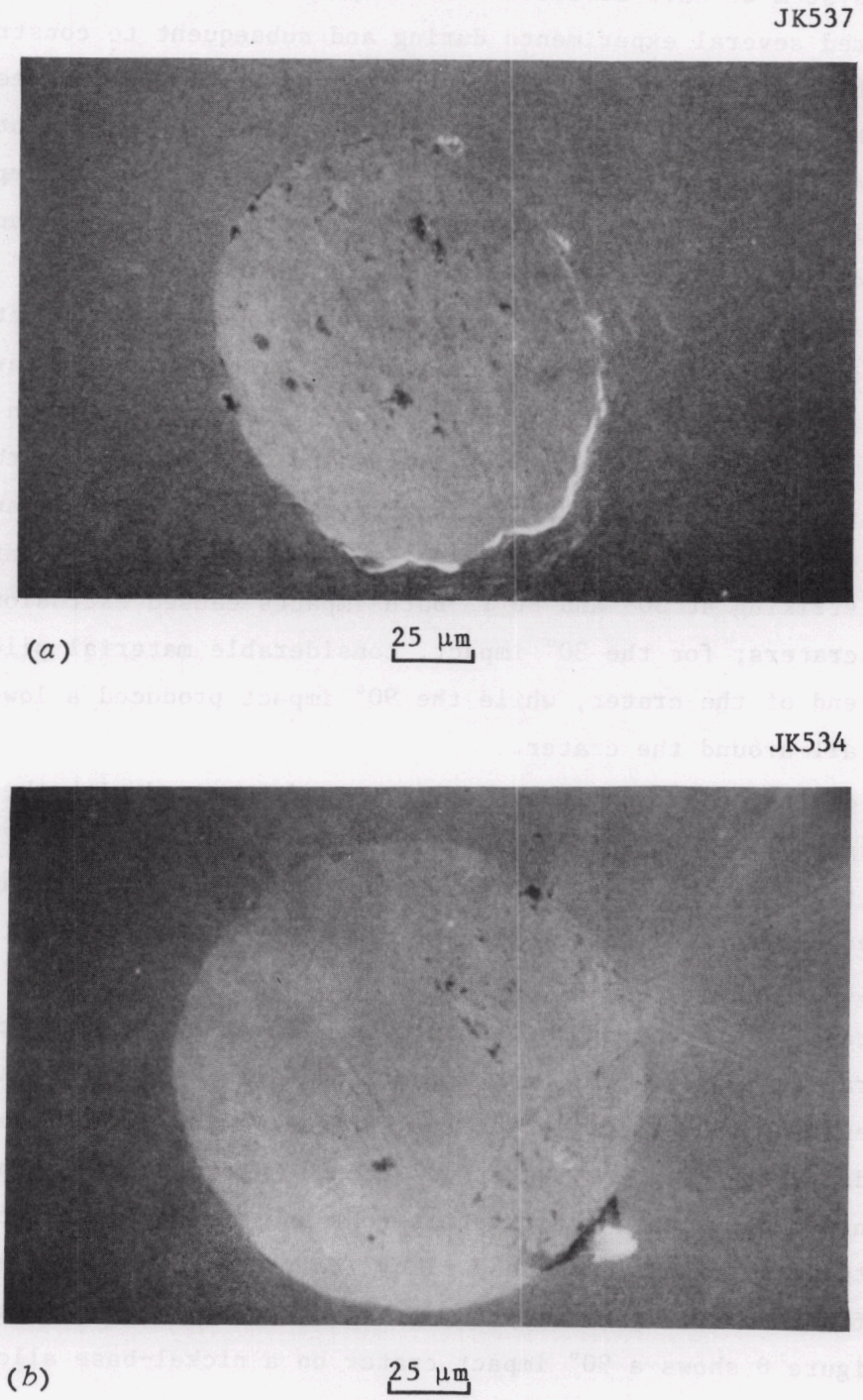

Fig. 6. Craters formed in 4340 steel at room temperature by impacts of spheres traveling 30 m/s with impact angles of (*a*) 30° and (*b*) 90°.

JK542

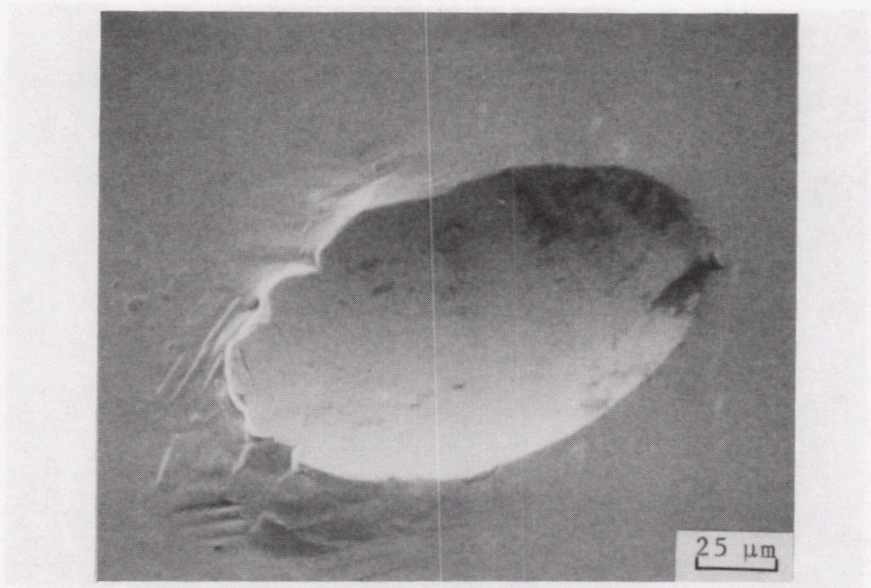

(*a*)

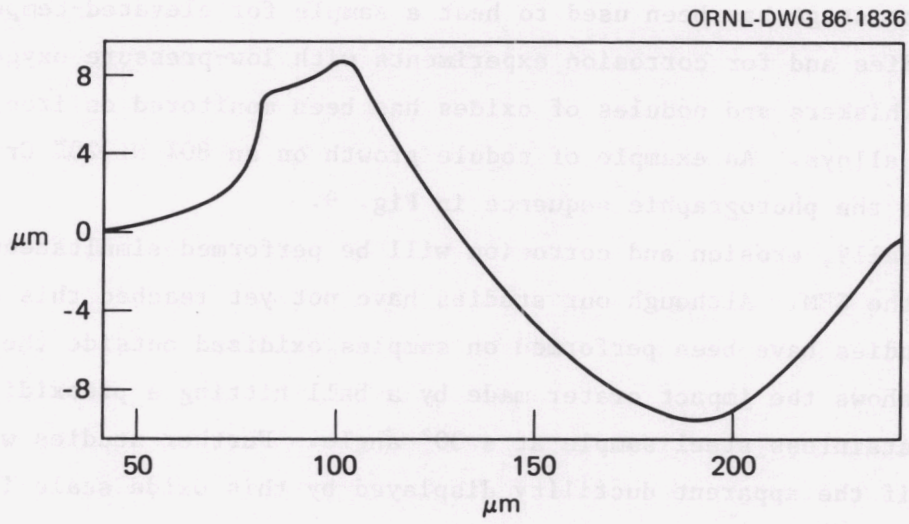

(*b*)

Fig. 7. (*a*) Secondary electron image and (*b*) profilometer trace for an impact crater formed on Berylco 25 by the 30°-angle impact of a tungsten carbide ball at 30 m/s.

JK555

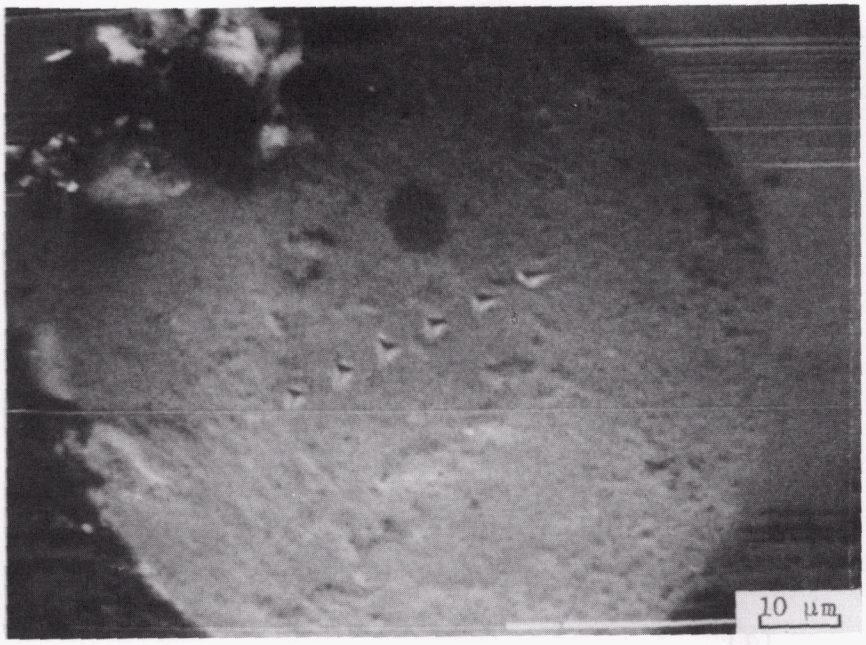

Fig. 8. Impact crater on Hastelloy C-276 formed by 90° impact of tungsten carbide ball traveling about 30 m/s. Indentations formed during hardness measurements with the Nanoindenter are shown in the crater.

The hot stage has been used to heat a sample for elevated-temperature impact studies and for corrosion experiments with low-pressure oxygen. The growth of whiskers and nodules of oxides has been monitored on iron, nickel, and cobalt alloys. An example of nodule growth on an 80% Ni–20% Cr alloy is shown in the photographic sequence in Fig. 9.

Eventually, erosion and corrosion will be performed simultaneously on a sample in the SEM. Although our studies have not yet reached this stage, erosion studies have been performed on samples oxidized outside the SEM. Figure 10 shows the impact crater made by a ball hitting a preoxidized type 304L stainless steel sample at a 30° angle. Further studies will determine if the apparent ductility displayed by this oxide scale is typical for impact and oxidation conditions.

SUMMARY

A unique system has been constructed to perform erosion and erosion-corrosion studies in a specially modified SEM. This microscope incorporates a gun that shoots particles at a target specimen in the SEM and a

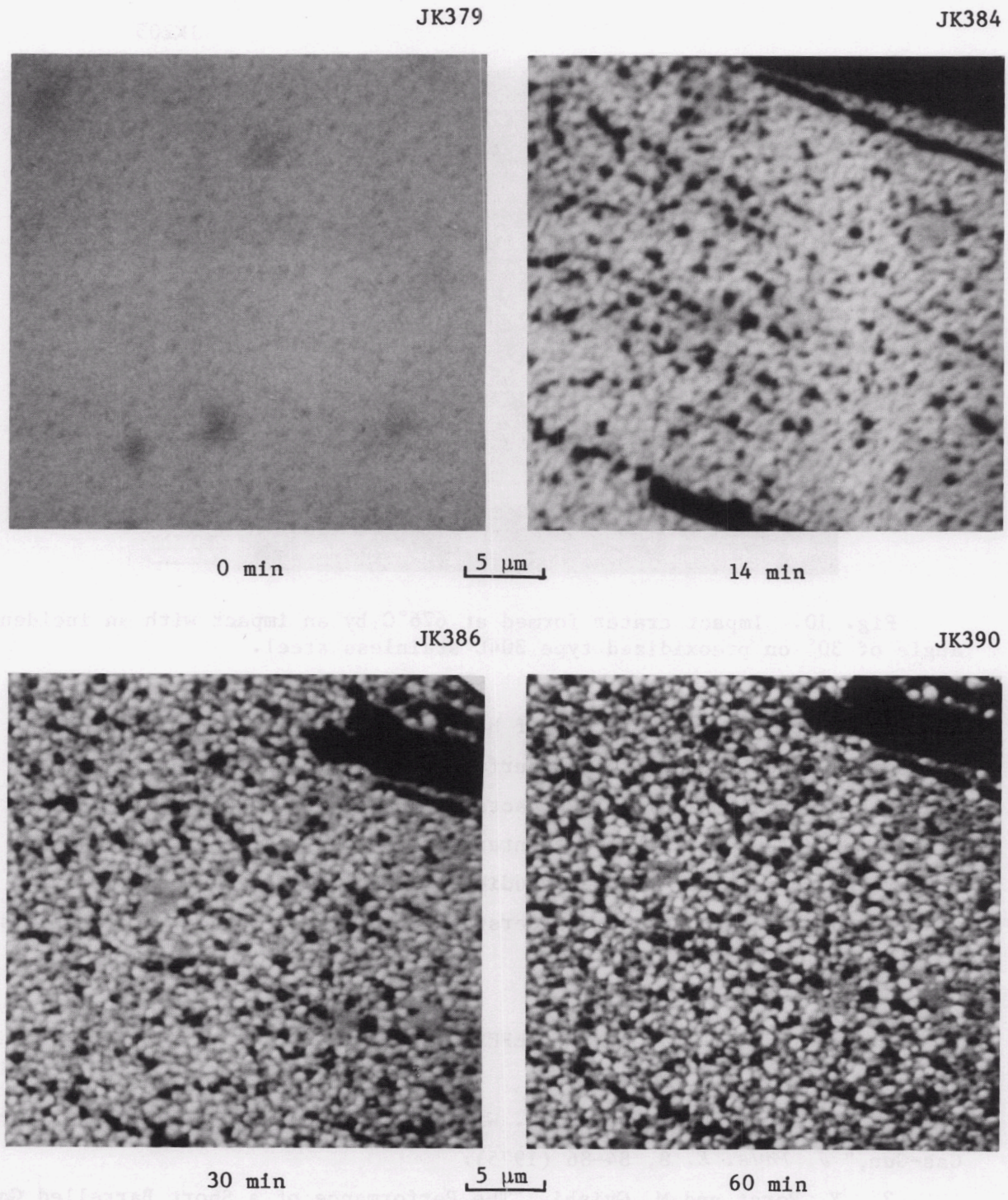

Fig. 9. Example of the formation and coarsening of oxides on 80% Ni–20% Cr sample oxidized at 560°C in about 6×10^{-5} atm oxygen.

JK205

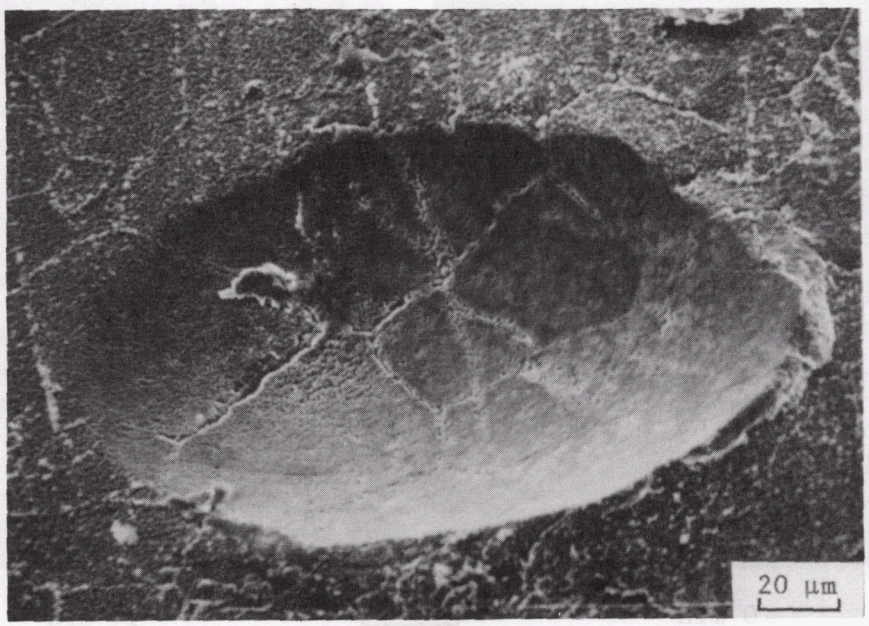

Fig. 10. Impact crater formed at 676°C by an impact with an incident angle of 30° on preoxidized type 304L stainless steel.

hot stage with the capabilities of heating both the specimen and the corrosive gas directed onto its surface. The premise is that the damage caused by single and multiple impacts of the particles can be related to erosion of alloys in systems of interest. Our initial results show that the system is capable of novel studies of erosion and erosion-corrosion, which should lead to improved understanding of those methods of materials degradation.

REFERENCES

1. I. M. Hutchings and R. E. Winter, "A Simple Small-Bore Laboratory Gas-Gun," *J. Phys. E.* **8**, 84–86 (1975).

2. Y. Porat and M. Gvishi, "The Performance of a Short Barrelled Gas Gun," *J. Phys. E.* **13**, 504–05 (1980).

3. A. A. Lakhani, D. Urech, and M. Mattingly, "High Temperature Substage for a Scanning Electron Microscope," *Rev. Sci. Instrum.* 55(6), 925–7 (1984).

4. S. K. Verma, G. M. Raynaud, and R. A. Rapp, "Hot-Stage Scanning Electron Microscope for High-Temperature In-Situ Oxidation Studies," *Oxid. Met.* 15(5/6), 471–83 (1981).

5. J. E. Castle and M. R. Hunt, "In-Situ Oxidation of Iron and Steel in the Scanning Electron Microscope," *Corr. Sci.* **16**, 137–44 (1976).

6. A. M. Brown and P. L. Surman, "Oxidation of Iron Within the Scanning Electron Microscope: Oxide Crystallite Growth Kinetics During the Oxidation of Iron in CO_2," *Surf. Sci.* **52**, 85–102 (1975).

7. J. R. Keiser and P. J. Ficalora, "Effects of the Impact of Small Hard Spheres on Ductile Metals," *Microstruct. Sci.* **13**, 237–46 (1986).

8. J. B. Pethica, *Ion Implantation into Metals*, ed. V. Ashworth, W. Grant, and R. Procter, Pergamon Press, Oxford, 1982, pp. 147–56.

INTERNAL DISTRIBUTION

1–2. Central Research Library
3. Document Reference Section
4–5. Laboratory Records Department
6. Laboratory Records, ORNL RC
7. ORNL Patent Section
8. T. M. Besmann
9–11. R. A. Bradley
12. A. J. Caputo
13. P. T. Carlson
14. J. H. DeVan
15. J. R. DiStefano
16. J. C. Griess
17. M. Howell
18. H. S. Hsu
19. R. R. Judkins
20–24. J. R. Keiser
25. J. M. Leitnaker
26. E. L. Long, Jr.
27. C. J. McHargue
28. W. C. Oliver
29. A. R. Olsen
30. R. E. Pawel
31. G. M. Slaughter
32. J. O. Stiegler
33–35. P. T. Thornton
36. P. F. Tortorelli
37. C. S. Yust
38. R. J. Charles (Consultant)
39. G. Y. Chin (Consultant)
40. H. E. Cook (Consultant)
41. Alan Lawley (Consultant)
42. W. D. Nix (Consultant)
43. R. L. Smith (Consultant)
44. J. C. Williams (Consultant)

EXTERNAL DISTRIBUTION

45. BATTELLE COLUMBUS LABORATORIES, 505 King Avenue, Columbus, OH 43201

    I. G. Wright

46–48. ELECTRIC POWER RESEARCH INSTITUTE, 3412 Hillview Avenue, P.O. Box 10412, Palo Alto, CA 94303

    W. T. Bakker
    R. I. Jaffee
    J. Stringer

49. EXXON RESEARCH AND ENGINEERING COMPANY, P.O. Box 101, Florham Park, NJ 07932

    G. Sorell

50–51. GENERAL ELECTRIC COMPANY, 1 River Road, Schenectady, NY 12345

    H. von E. Doering
    R. W. Haskell

52. LAWRENCE BERKELEY LABORATORY, University of California, Berkeley, CA 94720

    A. V. Levy

53. THE METAL PROPERTIES COUNCIL, INC., United Engineering Center, 345 E. Forty-Seventh Street, New York, NY 10017

A. O. Schaefer

54. NATIONAL BUREAU OF STANDARDS, Materials Building, Gaithersburg, MD 20899

L. K. Ives

55. NORTH CAROLINA STATE UNIVERSITY, Materials Engineering Department, Raleigh, NC 27659

H. Conrad

56. PENNSYLVANIA STATE UNIVERSITY, 167 Materials Research Laboratory, University Park, PA 16802

N. H. McMillan

57. STAL-LAVAL TURBIN AB, Finspong S-61220, Sweden

S. Jansson

58–59. THE OHIO STATE UNIVERSITY, Department of Metallurgical Engineering, 116 W. 19th Avenue, Columbus, OH 43210

R. A. Rapp
P. Shewmon

60. UNIVERSITY OF CALIFORNIA, BERKELEY, Department of Mechanical Engineering, Berkeley, CA 94720

J. A. C. Humphrey

61. UNIVERSITY OF CAMBRIDGE, Department of Metallurgy, Pembroke Street, Cambridge, England

I. M. Hutchings

62. UNIVERSITY OF CINCINNATI, Department of Aerospace Engineering and Applied Mechanics, Cincinnati, OH 45221

W. Tabakoff

63. UNIVERSITY OF NOTRE DAME, Department of Metallurgical Engineering and Materials Science, P.O. Box E, Notre Dame, IN 46556

T. H. Kosel

64. DOE, ENERGY CONVERSION AND UTILIZATION TECHNOLOGIES DIVISION, Forrestal Building, Washington, DC 20585

J. J. Eberhardt

65. DOE, MORGANTOWN ENERGY TECHNOLOGY CENTER, P.O. Box 880, Morgantown, WV 26505

J. M. Hobday

66. DOE, OAK RIDGE OPERATIONS OFFICE, P.O. Box E, Oak Ridge, TN 37831

Assistant Manager for Energy Research and Development

67. DOE, OFFICE OF BASIC ENERGY SCIENCES, Materials Sciences Division, Washington, DC 20545

F. V. Nolfi, Jr.

68–74. DOE, OFFICE OF FOSSIL ENERGY, Washington, DC 20545

J. P. Carr
S. J. Dapkunas (5)
T. B. Simpson

75. DOE, OFFICE OF VEHICLE AND ENERGY R&D, Forrestal Building, Washington, DC 20585

R. B. Schulz

76. DOE, PITTSBURGH ENERGY TECHNOLOGY CENTER, P.O. Box 10940, Pittsburgh, PA 15236

S. R. Lee

77–104. DOE, TECHNICAL INFORMATION CENTER, P.O. Box 62, Oak Ridge TN 37831

For distribution by microfiche as shown in DOE/TIC-4500, Distribution Categories UC-90 (Coal Conversion and Utilization) and UC-90h (Materials and Components).